Available online at www.sciencedirect.com
SCIENCE DIRECT®

Journal of the European Ceramic Society 23 (2003) 2777–2785

www.elsevier.com/locate/jeurceramsoc

Glass and metals on crystalline oxides

N. Ravishankar[1], Shelley R. Gilliss, C. Barry Carter*

Department of Chemical Engineering and Materials Science, University of Minnesota, 421 Washington Avenue S.E., Minneapolis MN 55455, USA

Abstract

Wetting and dewetting of liquid metals and glasses on ceramic substrates has been investigated using a combination of microscopy techniques. The influence of surface structure on dewetting behavior and the influence of the dewet droplets on the morphology of surface steps has been shown with the aid of experimental observations from many systems. The role of chemistry and kinetics on the wetting behavior has also been demonstrated. Finally, the possibility of exploiting reconstructed ceramic surfaces for nanopatterning of metal particles has been illustrated.

Keywords: Alumina; Ceramic surfaces; Dewetting; Nanopatterning; Wett behavior

1. Introduction

The wetting of a ceramic phase by a glassy phase or by a liquid metal is a technologically relevant problem that is encountered under many situations. Processing of ceramics using liquid phase sintering relies on the wetting of the ceramic powder compact by a lower melting additive.[1–3] The additive may be a non-metallic glassy phase, as in oxide ceramics, or can be a liquid metal as in the case of Co additives for WC ceramics. The wetting of ceramics by liquid metals is also encountered in joining applications like active metal brazing.

While there are many common features in the wetting behavior of glasses and metals on ceramic surfaces, there remain distinct differences. Wetting behavior of a liquid on a substrate is usually quantified in terms of the contact angle that the liquid makes with the substrate material. Analysis of sessile droplet geometry is the most commonly used method to obtain contact angles and study wetting behavior. Alternatively, dewetting of an initially continuous film has also been shown to be a powerful approach to study several aspects of glass/ceramic interactions. While the effect of atmosphere can play an important role in the wetting behavior of glasses, it is probably more critical in the case of liquid metals.

The main purpose of this paper is to review our work on dewetting behavior in a wide variety of metal and ceramic systems and identify common themes that link these systems together. Thus, the results from different systems are combined into sections based on the common features rather than focusing on system-specific details.

2. Background

2.1. Metal/ceramic interfaces

Metal/ceramic interfaces are encountered in a wide variety of systems. The joining of metals and ceramics by active metal brazing relies on the wetting of the ceramic by a liquid metal. In the electronics industry, the packaging of microelectronic devices places metals and ceramics in intimate contact and the reliability of the device often depends upon the integrity of the metal/ceramic interface. Ceramics are also used as barrier coatings (thermal or reaction barriers) on metals surfaces that are susceptible to corrosion/reaction at high temperatures. Another application that has gained importance more recently is in the field of implant materials. In this case, bioactive ceramics (bioglass or hydroxyapatite) are coated on Ti alloys and the integrity of the interface dictates the performance of the material inside the human body. Oxide-dispersion strengthened metals represent examples where an oxide phase in a finely dispersed form is used to strengthen the matrix metal. Depending on the application, different requirements need to be met. While the formation of reaction products that aid

* Corresponding author. Tel.: +1-612-625-8805; fax: +1-612-626-7246.
E-mail address: carter@cems.umn.edu (C.B. Carter).
[1] Present address: Materials Research Center, Indian Institute of Science, Bangalore 560 012, India.

0955-2219/03/$ - see front matter © 2003 Elsevier Ltd. All rights reserved.
doi:10.1016/S0955-2219(03)00289-9

in bonding may be required for joining applications, reactions need to be prevented in the case of composite materials. Thus, it is important to understand the behavior of metals in contact with a ceramic material.

2.2. Glass/ceramic interfaces

The primary motivation to study glass/ceramic interfaces arises from the use of liquid-phase sintering for the processing of ceramics. The lower melting point additives that are used (usually silicates) are retained as a glass at room temperature and affect the properties of the materials. Identification and quantitative thickness measurements of intergranular glassy phases in ceramics have been topics of active experimental research and different types of behavior have been observed in different systems.[6,7] While oxide ceramics may have different thicknesses of the glass layers along different boundaries,[1,2] it is reported that the thickness of the intergranular phase in silicon nitride grain boundaries is independent of the crystallography.[8] Sintering in the presence of a liquid phase relies on the wetting of the ceramic compact by the liquid phase. Thus, it is important to study the wetting behavior of liquids in contact with a ceramic material.

3. Experimental

Pulsed-laser deposition (PLD) is used to deposit thin films (~100 nm) of the glass phases on single crystal surfaces of ceramics. Results from the $CaAl_2Si_2O_8/Al_2O_3$, $BaAl_2Si_2O_8/Al_2O_3$, SiO_2/TiO_2 and Bi_2O_3/ZnO systems are presented. For the dewetting studies, the film/substrate assembly is annealed for different times at temperatures where a liquid forms and cooled to room temperature at different rates. The Pt/Al_2O_3 system has been chosen for the metal/ceramic system. Two different types of samples are examined. A thin layer of Pt (~2 nm) dewets to produce small particles on the surface. This is used to study step interactions with particles. For dewetting studies, a small piece of Pt is placed on a reconstructed single crystal surface (m-plane) of alumina and annealed in vacuum at 1800 °C.

The annealed samples are examined at different length scales using a combination of microscopy techniques. Visible-light microscopy (VLM, Olympus BH2) is used to obtain overall droplet morphology over a large area. A field-emission scanning electron microscope (FESEM, Hitachi S900) operated at 5 kV has been used to examine interactions at a higher resolution. Samples for scanning electron microscopy (SEM) analysis were coated with a thin layer (~1–2 nm) of Pt to avoid charging. Topographic information at high resolution is obtained using an atomic force microscope (AFM, Nanoscope III) operated in contact mode.

Flux-growth of ceria samples was carried out using 99.9% pure (Alfa Aesar) ceria powder. Ten wt.% ceria powder was loaded in sodium tetraborate ($Na_2B_4O_7$) in a Pt crucible. The crucible was heat treated in air at 1150 °C for 72 h, cooled at a rate of 5 °C/h to 850 °C at which point the power to the furnace was shut off.

4. Results and discussion

4.1. Influence of particles on surface steps

The wetting behavior of liquids on flat surfaces is discussed in terms of the Young's equation that is based on the equilibrium of forces at the SLV triple junction.[9] In real systems, however, surfaces may not be ideally flat.[10] Single crystals of low energy orientations are the closest approximations to a truly flat surface and hence are often used to study the wetting behavior of liquids. However, most surfaces deviate slightly from the 'ideal' low-index orientation and hence reconstruct into a terrace-and-ledge morphology upon heat treatment at high temperatures.[11,12] The ledges/steps that are formed on the surface are usually mobile at high temperatures where the dewetting experiments are carried out.[13–16] Thus, interactions between the moving steps and the droplets at high temperatures become very important. The surface steps are modified by the presence of the droplets while the steps affect the morphology of the droplets they interact with.

Anorthite liquid dewets to forms circular droplets on a basal alumina surface. The details of dewetting on this surface have been extensively investigated.[17–19] Fig. 1 is a secondary-electron (SE) image of a basal surface of alumina that contained a dewet anorthite droplet. The droplet has been etched away using HF. The original position of the droplet is outlined by the surface steps here. The direction of motion of the surface steps has been indicated by the arrow. While steps further away from the droplet remain straight, step bending leading to the formation of curved steps is seen in the vicinity of the droplet. Another interesting feature that is seen here is the presence of faceted segments in regions that were lying beneath the droplet. These form as a result of precipitation of alumina from the anorthite liquid on cooling the sample. Accelerated kinetics due to the presence of a liquid leads to faceted step segments in this case.

This type of interaction of the steps with the particles on the surface is observed in many other systems.

Fig. 2 is a backscattered-electron (BSE) image showing steps interacting with a celsian particle. The celsian particle appears bright in this image due to its higher average atomic number. The pinning of steps on the surface is seen in this case. Extensive step bending leading to the formation of concentric step loops has been reported in this case.

Similar interaction leading to step bending and bunching has also been seen in the case of Pt particles lying on a basal alumina surface (Fig. 3). Step bending around large particles and the association of smaller particles with the step segments is shown here.

Fig. 4 is an illustration of a different system where such an interaction is encountered. The growth of single crystals of ceria from a supersaturated sodium tetraborate flux is shown here. The VLM image shown here is of a cerium oxide crystal grown from a supersaturated sodium tetraborate ($Na_2B_4O_7$) flux. Hopper growth is the cause for the spiraled morphology of this crystal. The depth of this pit is around 20 μm. After the first nuclei form, a dendritic growth stage occurs. "Hopper" growth usually follows this initial dendritic stage. Hoppers result when the growth rate at the edges exceeds that at the center of the crystal face.[20] This affect is further amplified when the crystal face resides at the

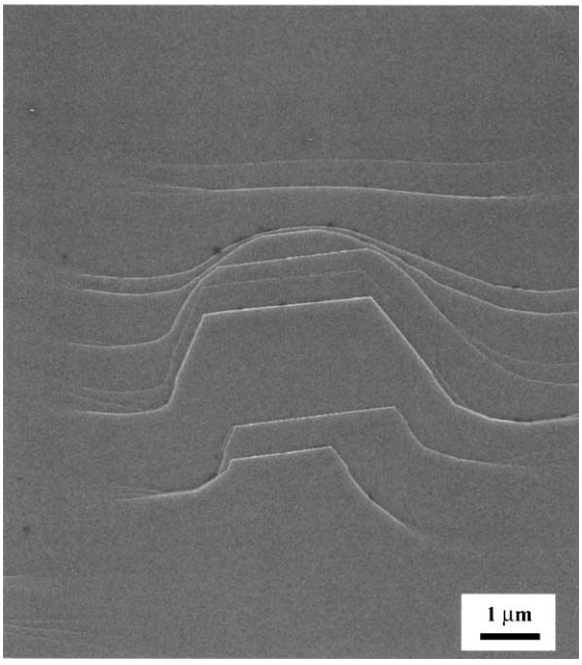

Fig. 1. SE image of the basal surface of alumina which contained anorthite droplets. The droplets have been etched away using HF, revealing faceted segments contained under the droplets of glass.

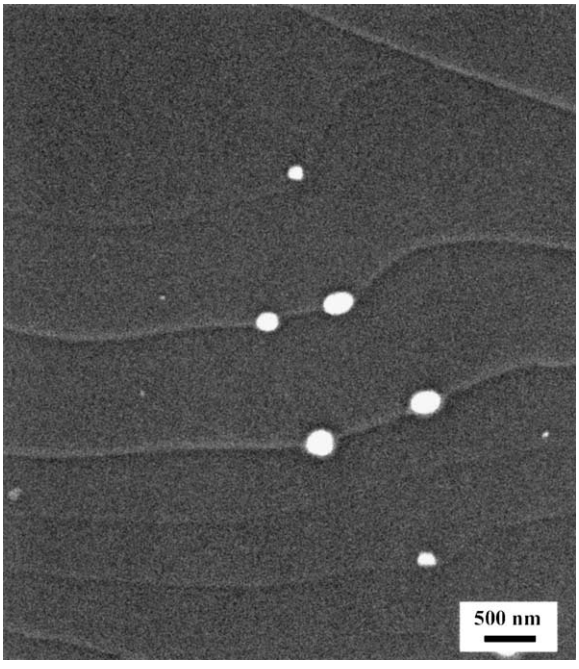

Fig. 2. BSE image of celsian particles on alumina. This image illustrates the pinning of steps by particles.

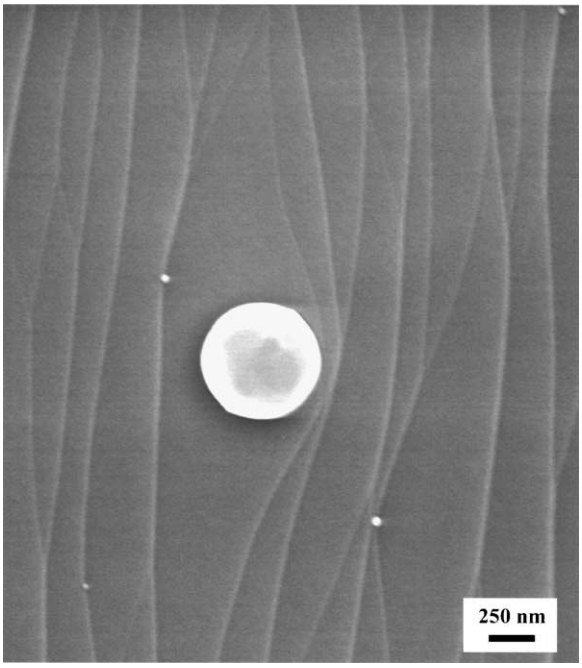

Fig. 3. SE image of a Pt particle pinning step motion on the basal surface of alumina.

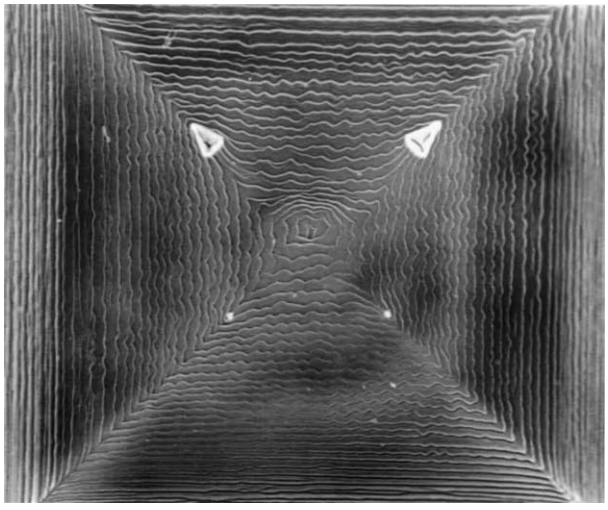

Fig. 4. VLM image of ceria grown by the flux-technique. The large spiral is due to hopper growth. These features are seen when crystals reside at the flux/air interface which inhibits solute transport to crystal at the interface. The area of the image is 1×1 mm.

surface of the flux (the case here) therefore restricting mass transport to this surface and causing such a structure. The bright, triangular shaped regions in Fig. 4 may be flux inclusions or remnants of the initial dendritic growth. Cerium oxide single-crystals grown in a sodium teraborate flux display a cube habit. The fastest growth direction is the $<111>$ leaving behind {001} faces. During runs where large amounts of flux have been lost, octahedron crystals bounded by {111} faces have been observed. This is in agreement with the observations of Linares where octahedron were only observed in the Na_2O–B_2O_3 system when $Na/B \leqslant 1.0$.[21]

An AFM image (deflection mode) of Bi_2O_3 crystallites on a (0001) ZnO surface is shown in Fig. 5. The crystalline particles impede the step motion leading to the formation of curved steps on this surface.

4.2. Influence of surface on the dewetting behavior

In the previous section, it was pointed out that the morphology of the dewet droplets is affected by the step structure. There have been extensive studies of morphological evolution in the case of anorthite liquid on reconstructed alumina surfaces.[4,5,22,23] It has been shown that the droplet morphology can deviate significantly from a circular cross-section due to the presence of a stepped structure.

Chemistry also plays a very important role on the development of the droplet morphology.[6,24] A striking example is seen in the VLM image of SiO_2 liquid dewetting on a (001) rutile surface (Fig. 6). Large dewet droplets of the order of 5–10 μm appear dark in this image. Smaller droplets that form a cellular network can be seen around the larger dewet droplets. Dewetting on this surface leads to the formation of droplets with two distinct length scales. The inset shows an interesting contrast variation inside the larger dewet droplet. The origin of this contrast is discussed later. The formation of complex non-circular patterns of the dewet droplets in this case is related to the instabilities arising due to solute transport. The detailed mechanism for the formation of such structures has been discussed elsewhere[25] and is outlined here. Dewetting of the liquid on the (001) surface begins with the formation of local regions in the liquid differing in thickness and curvature. The difference in curvature leads to differences in local solute chemical potential as given by the Gibbs–Thomson equation. Thus, redistribution of solute that takes place across regions with different thickness/curvature leading to local changes in composition/wetting behavior. Thus, any instability at the periphery of the liquid can be amplified leading to the formation of such complex patterns. This is analogous to the growth of dendritic structures during solidification.

A direct evidence for the mass transport occurring across the regions of different thickness is seen in the TEM image shown in Fig. 7. This cross section sample was prepared using a focused-ion beam tool. The Pt strap seen coating the cross-section in Fig. 7 is deposited to protect the specimen during the thinning process. Diffusion of solute across the droplet leads to an enrichment near the periphery of the droplet. Depending on the temperature, the excess solute precipitates out from the liquid phase. The arrows in the figure indicate regions on the substrate where the excess TiO_2 has precipitated indicating an enrichment of the solute phase towards the periphery of the droplet. This precipitated region has a radial symmetry and leads to the contrast variation that was shown in the inset in Fig. 6.

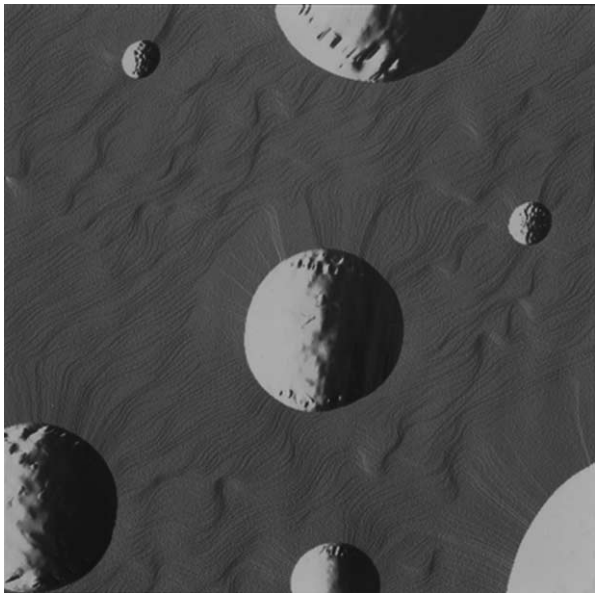

Fig. 5. AFM deflection-mode image of Bi_2O_3 crystallites on (0001) ZnO surface. These crystalline particles impede step motion which causes curved steps on the surface. The image scan size is 20×20 μm.

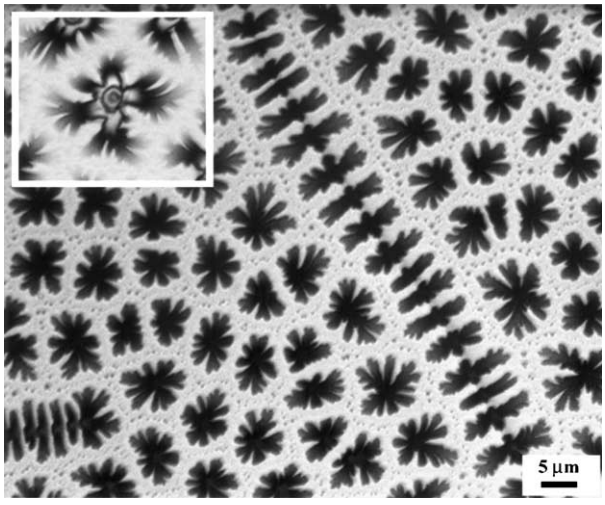

Fig. 6. VLM image of SiO_2 which has dewet the (001) surface of rutile. Dewetting on this surface occurs on two length scales.

Fig. 7. Cross-sectional TEM image of SiO_2 dewet droplets on the (001) surface of rutile. Diffusion of solute across the droplet results in ridges forming at the periphery of the droplet (indicated by arrows).

Another interesting variation is observed during dewetting of SiO_2 on a (110) surface of rutile. Fig. 8 is a deflection AFM image showing dewet SiO_2 droplets on a (110) surface of rutile. The reconstruction of the (110) surface of rutile under UHV conditions has been extensively studied.[26–29] Here, the surface reconstructs to form small steps of the order of 2 nm. The presence of these steps on the surface lead to the formation of elongated droplets, aligned along the step direction.

4.3. Influence of kinetics on morphological evolution : cooling rate effects

The influence of structural features like surface steps and chemistry on the evolution of dewet droplet morphology was discussed in the previous sections. In this section, the influence of the cooling rate on the droplet morphology is discussed.

Fig. 9 is an SE image of the m-plane of alumina on which an initially continuous layer of anorthite has dewet to form discrete droplets. The sample was cooled at 1 °C/min. Nominal cooling rates of the order of 200 °C/min lead to the formation of non-circular droplets that are flattened parallel to the step direction on one side. Slow cooling leads to the attainment of equilibrium along the periphery of the droplet. The liquid is seen to spread along one type of facet on the reconstructed m-plane. This situation is analogous to secondary wetting that is seen in the case of liquids dewetting on polycrystalline substrates.

The effect of cooling rate is very pronounced in the case of SiO_2 liquid on the (001) rutile surface. It is possible to suppress dewetting in this case by quenching the sample. Fig. 10 shows a VLM image from a sample that was annealed at 1650 °C for 15 min and removed from the furnace. The high rate of cooling achieved by this process suppresses the dewetting of the continuous liquid film. Two distinct length scales for the fluctuation can be seen in this case. Reheating the sample to 1650 °C and cooling it slowly leads to the formation of the patterns that were shown in Fig. 6. This is seen in the VLM image shown in Fig. 11. The fluctuations on the liquid

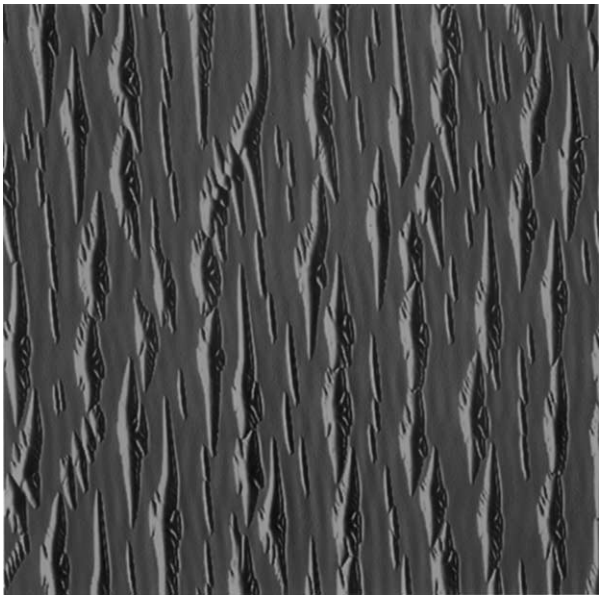

Fig. 8. AFM deflection-mode image of SiO_2 droplets on the (110) surface of rutile. The presence of steps on the surface leads to the formation of elongated droplets. The image scan size is 50×50 μm.

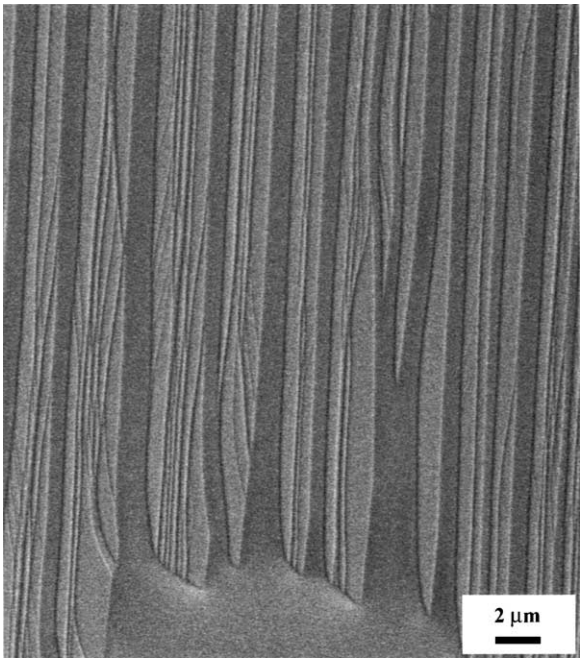

Fig. 9. SE image of anorthite glass which has dewet the m-plane of alumina. The liquid has spread along one type of facet on the reconstructed surface.

surface are precursors to the two length scales of dewet droplets that are observed on this surface.

4.4. Reprecipitation behavior: homogeneous vs heterogeneous precipitation

As pointed out earlier, the condition of an inert substrate is often not realized in practice and the substrate actively participates in the wetting/dewetting process. In particular, in the examples presented here, the liquid dissolves the underlying substrate at high temperature, then reprecipitates on cooling the sample. In the case of the alumina/anorthite system, a pseudobinary system, the reprecipitation takes place heterogeneously on the existing substrate. The faceted steps that are seen in Fig. 1 are formed as a result of the reprecipitation process.

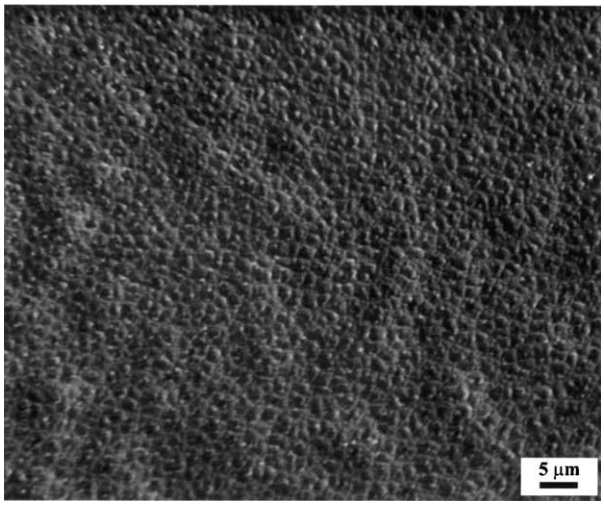

Fig. 10. VLM image of SiO_2 on the (001) rutile surface. This sample has been quenched from 1650 °C, suppressing dewetting.

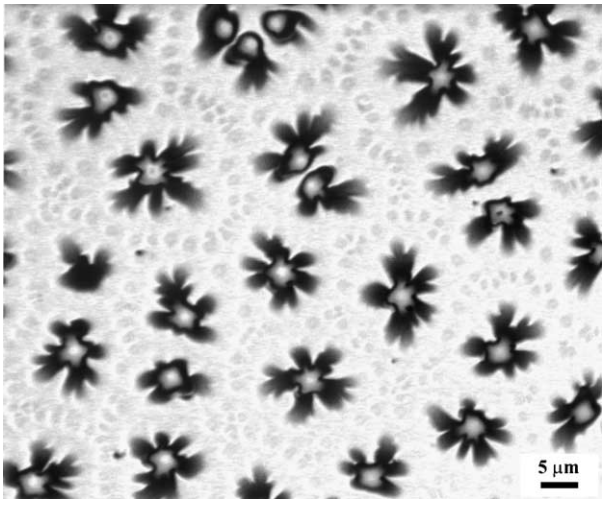

Fig. 11. VLM image of the sample from Fig. 10 which has been reheated to 1650 °C and cooling slowly, leading to pattern formation.

Fig. 12 is a BSE image showing a dewet SiO_2 droplet on a (001) rutile surface. The SiO_2-rich liquid that has a lower average atomic number appears darker in this image. Fine precipitates (that appear brighter) are seen on the surface of the dewet droplet. From the phase diagram for the TiO_2–SiO_2 system, TiO_2 dissolves in the SiO_2 liquid at high temperatures. The excess TiO_2 reprecipitates on cooling. In the alumina/anorthite case, it was seen that the reprecipitation takes place heterogeneously on the existing alumina substrate. However, in this case, homogeneous precipitation of the TiO_2 phase is also observed. It is to be noted that this process does not rule out the precipitation of TiO_2 by heterogenoeus nucleation.

However, in the case of TiO_2 precipitating from a SiO_2-rich liquid, the reprecipitation also takes place homogeneously in the liquid phase. The amount of homogeneous versus heterogeneous nucleation may be determined by the undercooling and hence a large difference is seen in samples processed at different cooling rates.

Fig. 13 is a BSE from a bicrystal of rutile containing a thick layer of SiO_2 glass in between. The fabrication of such bicrystals has been shown to be very useful in the study of grain boundary migration in bicrystals. GBM is observed in this particular boundary implying that mass was transported from one of the bounding faces of rutile to the other. This implies a heterogeneous nucleation of the rutile phase. The precipitation of TiO_2

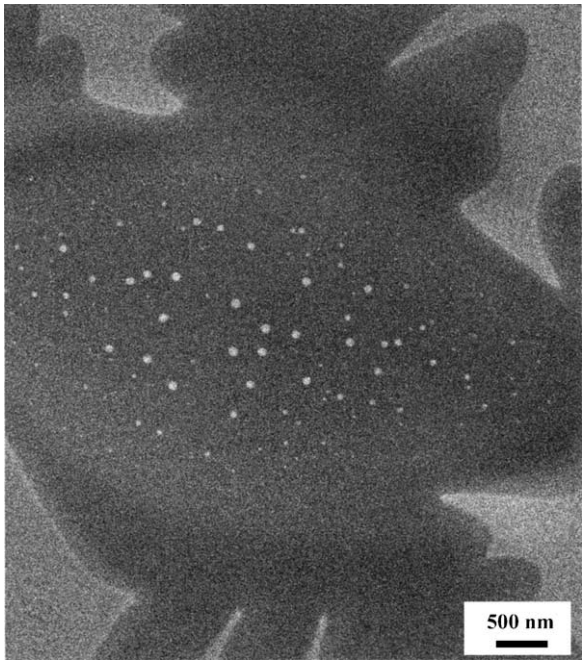

Fig. 12. BSE image of SiO_2 on the (001) surface of rutile. Fine precipitates (appear bright) are present on the surface of the dewet droplet indicating homogeneous nucleation is occurring during cooling.

rich phase is seen in the central region of the glassy phase implying that a homogeneous precipitation of the TiO_2-rich phase has taken place inside the glass layer. Thus, in this case, both homogeneous and heterogeneous nucleation of the TiO_2 phase takes place.

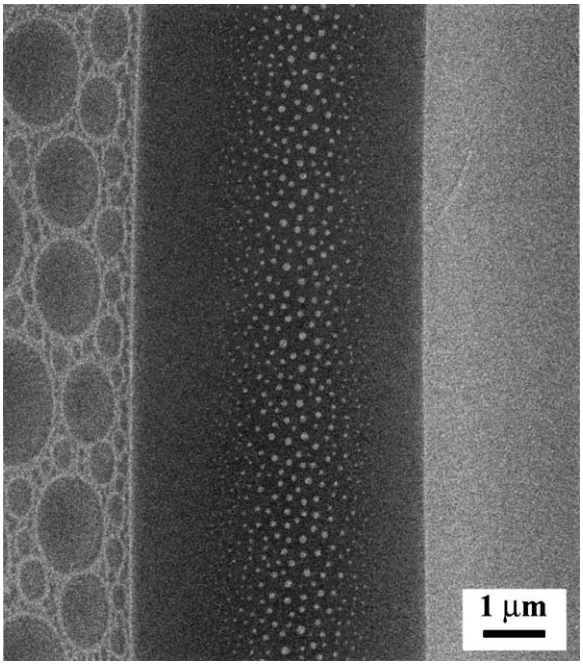

Fig. 13. BSE image of a bicrystal of rutile which contains a thick layer of SiO_2 in between. GBM is observed in this bicrystal, indicating heterogeneous nucleation occurs, however the fine precipitates seen in the central region between the two rutile crystals also indicates homogeneous nucleation.

4.5. Pt on m-alumina: nanopatterning on a stepped surface

The wetting behavior of metals on ceramic substrates has been investigated in great detail for a wide variety of systems. The influence of surface reconstruction on the wetting behavior of ceramics has been investigated. Here, the possibility of using reconstructed ceramic surfaces to produce patterned metal nanoparticles has been demonstrated. Ordered arrays of metal nanoparticles find applications ranging from catalysis to magnetic materials and thus are important technologically.

Fig. 14 is an SE image from a Pt droplet on a reconstructed m-plane of alumina that was heat treated at 1800 °C for 15 min in a vacuum furnace. The Pt forms a liquid at high temperatures and solidifies to form a dendritic morphology as seen in this image. The size of the particle is of the order of 250 μm. Examination of regions adjacent to the droplet shows the possibility of using the m-plane for nanopatterning. Fig. 15 is an SE image from a regions adjacent to a larger Pt droplet. Nanoparticles of Pt in the form of ordered arrays can be seen in this image. The particles are located on the crests of the stepped structure. The striking feature is the uniformity in size and spacing between the particles. The particles form by condensation of liquid from the vapor phase. The propensity for the particles to lie on the crests of the stepped structure implies that condensation is favored in these regions. Capillary surface tension forces alone cannot explain this observation. There may be an electrostatic origin to the formation of the liquid phase along the crest regions. Presence of a continuous layer of liquid along the crest can then lead to the

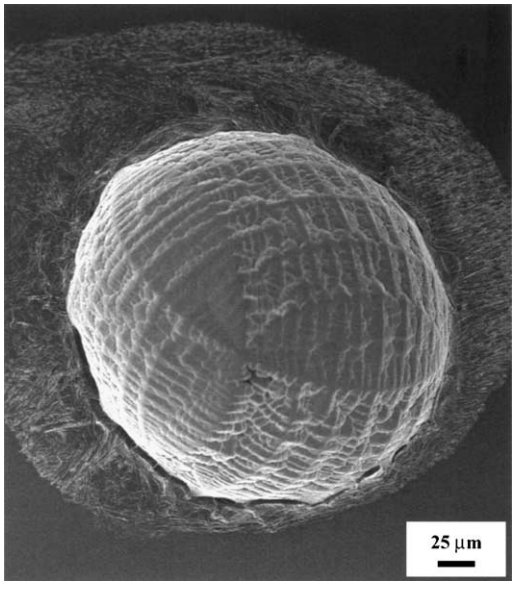

Fig. 14. SE image of a Pt droplet on a reconstructed surface of m-plane alumina. The Pt which was liquid has solidified to form a dendritic morphology. The particle is approximately 250 μm in diameter.

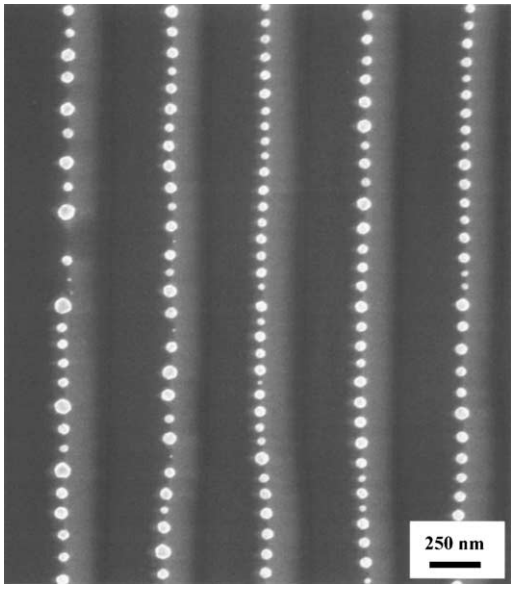

Fig. 15. SE image of Pt nanoparticle arrays on the reconstructed surface of m-plane alumina. This image was taken in a region near the large particle in Fig. 14.

formation of such ordered arrays due to a Rayleigh-type instability. The wavelength of the instability dictates the spacing between the particles. This approach opens up newer ways to produce such ordered arrays.

5. Conclusions

Several conclusions can be drawn based on the results presented here.

- While the wetting behavior of liquid metals and silicate glass on ceramic substrates represent two very different systems, there are common features associated with these systems.
- There is a two-way interaction between the dewet droplets and the steps on the surface. While the presence of steps affect the morphology of dewet droplets, the presence of droplets affect the motion of steps on the surface.
- Kinetics plays a crucial role in determining the dewetting behavior. For the case of anorthite liquid on m-plane alumina, slow cooling leads to extensive spreading of the liquid along one type of facet on the surface. Fast cooling suppresses dewetting in the case of silica liquid on a rutile surface.
- The substrate actively participates in the dewetting process. In the case of anorthite liquid on alumina, alumina dissolves in the liquid at high temperatures. The excess alumina precipitates heterogeneously on the substrate on cooling. In the case of silica on rutile surface, the excess TiO_2 that dissolves in the silica liquid also precipitates out homogeneously in the liquid. The redistribution of silica in this case also leads to the formation of patterns that are observed in this case.
- It is possible to use reconstructed ceramic surfaces as templates to produce arrays of metal nanoparticles. This has been demonstrated experimentally for the case of Pt particles on alumina substrates.

Acknowledgements

This research has been supported by the US Department of Energy through grants DE-FG02-92ER45465-A004 and DE-FG02-01ER45883. The authors would like to acknowledge Professor Stan Erlandsen at the Department of Cell Biology and Neuroanatomy, University of Minnesota for access to the FESEM, Chris Frethem for technical assistance. Stimulating discussions with Dr. S. Ramamurthy, Dr. M.P. Mallamaci, Professor H. Schmalzried, Dr. Joe Michael and Dr. Paul Kotula are gratefully acknowledged.

References

1. Clarke, D. R., Grain boundaries in polycrystalline ceramics. *Ann. Rev. Mater. Sci.*, 1987, **17**, 57–74.
2. Clarke, D. R., *Intergranular Phases in Polycrystalline Ceramics, in Surfaces and Interfaces of Ceramic Materials*. Kluwer Academic Publishers, Dordrecht, 1989.
3. German, R. M., *Sintering Theory and Practice*. John Wiley and Sons, New York, 1996.
4. Ramamurthy, S., Hebert, B. C. and Carter, C. B., Dewetting of Glass-Coated {1010} α-Al_2O_3 Surface. *Phil. Mag. Lett.*, 1995, **72**, 269–275.
5. Ramamurthy, S., Herbert, B. C., Carter, C. B. and Schmalzried, H., In *Interaction of Silicate Liquid with Sapphire Surfaces*, Boston, 1996, pp. 295–300.
6. Kouh Simpson, Y. M., Carter, C. B., Sklad, P. and Bentley, J., In *Grain Boundary Glassy Phase Identification and Possible Artifacts*, 1986, pp. 427–434.
7. Mallamaci, M. P., Bentley, J. and Carter, C. B.. In *Mat. Res. Soc. Symp. Proc.; Vol. 285*, ed. B. Braren, J. Dubowski and D. Norton. Materials Research Society, Pittsburgh, PA, 1992, pp. 433–438.
8. Cinibulk, M. K., Kleebe, H.-J., Schneider, G. A. and Rühle, M., Amorphous intergranular films in silicon nitride ceramics quenched from high temperatures. *Journal of the American Ceramic Society*, 1993, **76**, 2801–2808.
9. Young, T., An essay on the cohesion of fluids. *Phil. Trans. Roy. Soc. London*, 1805, **95**, 65–87.
10. Saiz, E., Tomsia, A. P. and Cannon, R. M., Ridging effects on wetting and spreading of liquids on solids. *Acta. Mater.*, 1998, **46**, 2349–2361.
11. Heffelfinger, J. R., Bench, M. W. and Carter, C. B., On the faceting of ceramic surfaces. *Surf. Sci. Lett.*, 1995, **343**, 1161–1166.
12. Heffelfinger, J. R. and Carter, C. B., Mechanisms of surface faceting and coarsening. *Surf. Sci.*, 1997, **39**, 188–200.
13. Ramamurthy, S., Mallamaci, M. P., Zimmerman, C. M., Carter, C. B., Duncombe, P. R. and Shaw, T. M., Microstructure of polycrystalline MgO penetrated by a silicate liquid. *Microscopy & Microanalysis*, 1996, **2**, 113–128.
14. Ravishankar, N. and Carter, C. B., Exuding liquid from grain boundaries in alumina. *J. Am. Ceram. Soc.*, (2000) (communicated).
15. Ravishankar, N. and Carter, C. B., *Migration of Silicate Liquids out of Grain Boundaries in Ceramics*. Portland, OR, Springer, 1999.
16. Ravishankar, N., Carter, C. B., Bunching of surface steps and facet formation on alumina Surface. *J. Mater. Res.*, (2002).
17. Mallamaci, M. P., Bentley, J. and Carter, C. B., In-situ TEM crystallization of silicate–glass films on Al_2O_3. *Acta Mater.*, 1998, **46**, 283–303.
18. Mallamaci, M. P. and Carter, C. B., Faceting of the interface between Al2O3 and anorthite glass. *Acta Mater.*, 1997, **46**, 2895–2907.
19. Mallamaci, M. P. and Carter, C. B., Crystallization of pseudo-orthorhombic anorthite on basal sapphire. *J. Am. Ceram. Soc.*, 1999, **82**, 33–42.
20. Pamplin, B. R., *Crystal Growth*. Pergamon, Oxford, 1975.
21. Linares, R. C., Growth and properties of CeO2 and ThO2 single crystals. *J. Phys. Chem. Solids*, 1967, 1285–1291.
22. Simpson, Y. K. and Carter, C. B., Faceting behavior of alumina in the presence of a glass. *J. Am. Ceram. Soc.*, 1990, **73**, 2391–2398.
23. Ramamurthy, S., Herbert, B. C., and Carter, C. B., *Non-Equilibrium Silicate Glass in Contact with Faceted {1010} α-Al2O3 Surface: An SEM Study*, Kansas City, 1995, pp. 340–341.
24. Ramamurthy, S., Mallamaci, M. P., Zimmerman, C. M., Sartain,

K. B. and Carter, C. B., *Glass Crystallization and Interfaces*. Materials Science Forum, 1995 pp. 753–756.
25. Ravishankar, N., Gilliss, S. R., Carter, C. B. Pattern formation during dewetting of molten glass, *Phil. Mag. A*, (2002), (communicated).
26. Onishi, H. and Iwasawa, Y., Reconstruction of TiO2(110) surface: STM study with atomic-scale resolution. *Surface Science*, 1994, **313**, 1–2.
27. Murray, P. W., Condon, N. G. and Thornton, G., Na adsorption sites on TiO2(110) minus 1 multiplied by 2 and its 2 multiplied by 2 superlattice. *Surface Science*, 1995, **323**, 1–2.
28. Fischer, S., Munz, A. W., Schierbaum, K.-D. and Goepel, W., Geometric structure of intrinsic defects at TiO2(110) surfaces: an STM study. *Surface Science*, 1995, **337**, 1–2.
29. Diebold, U., Anderson, J. F., Ng, K.-O. and Vanderbilt, D., Evidence for the tunneling site on transition-metal oxides: TiO2(110). *Physical Review Letters*, 1996, **77**, 1322–1325.